

Effects of Smoothed BRDF on Multi-angle Albedo Retrievals

Yanmin Shuai^{1,2,3,4}, Jian Yang^{1,*}, Junbo Duan¹, Latipa Tuerhanjiang^{2,3,5}, Chongyang Wang⁶ and Yu Ma⁷

¹ Liaoning Technical University, College of Surveying and Mapping and Geographic Science, 123000 Fuxin, China

² Xinjiang Institute of Ecology and Geography, CAS, 830011 Urumqi, China

³ Research Center for Ecology and Environment of Central Asia, CAS, 830011 Urumqi, China

⁴ University of Chinese Academy of Sciences, 100049 Beijing, China

⁵ Xinjiang University, 830046 Urumqi, China

⁶ Shenyang Gas Group Co. Ltd., 110000 Shenyang, China

⁷ RIOH Automobile Testing & Certification Technology Co. Ltd, 101103 Beijing, China

Abstract. BRDF as the intrinsic feature of surface targets, is an important parameter required by albedo inversion from multi-angle observations, especially for satellite data suit with less directional measurements. Several studies have shown up to introduce BRDF priori knowledge into albedo retrievals at different scale by spatial or temporal smoothing. Thus, it is necessary to further understand what's the influence induced by BRDF smoothing on albedo retrieval. This work investigated effects of smoothed BRDF on albedo magnitude through case studies over North America region using operational MCD43A&C BRDF products respectively smoothed in spatial and temporal scales. Our results show that BRDF of seasonal DBF samples smoothed from daily to monthly can lead to apparent relative difference to smoothed values of 10.97%, 9.42%, 8.24% and detectable absolute differences of 0.0172, 0.0095 and 0.0035 on related albedo respectively at Near Infrared, Short Wave and Visible broadband. The spatial smoothing of BRDF from 500m to 5600m results in relative differences to smoothed values of 17.38%, 14.38%, 27.23% and absolute differences of 0.0250, 0.0139, 0.0052 for the inversed albedo at above three broadbands.

1 Introduction

Albedo is defined as the ratio of reflected radiation to received solar radiation over surface target, which is an important parameter affecting the energy budget, thus contributing to the change of climate, land surface model and earth-atmosphere system[1-2]. Satellite remote sensing provides an effective potential way to estimate continuous land surface albedo in global or regional scale. Compared with previous single-angle estimation models, modern albedo algorithm relies on multiple-angle observations to first build BRDF(Bi-directional Reflectance Distribution Function), then integrate over incident and view hemispheres to calculate albedo. Studies pointed out that the relative errors can reach up to 45% in the albedo estimation without the consideration of angle effects[3-4].

The requirement of albedo accuracy keeps increasing with the need from various user communities or with the increasing of our understanding on the process of Earth system. The albedo accuracy of 0.02-0.05 is required by the community of global climate change, but increased to 0.02 for regional investigations[5-6]. Studies point out the magnitude of albedo varies with the change of land surface, and as well as related surrounding parameters in fine resolution[7-8]. Existing satellite-based operational

or sporadic albedo products span tens of meters to several kilometres in spatial scale and daily to annual phase in temporal scale, with different accuracy affected by inversion scheme, data quality, spatial or temporal resolution, etc[9-14]. Thus, it is important to further understanding the effect of factors induced the variation of albedo retrieval, for better service to user communities.

It is well known BRDF priori knowledge can improve the accuracy of albedo retrieval, especially for the estimation at high spatial resolution due to the lack of multi-angle observations. In recent years, BRDF smoothing process at spatial or temporal scale has been frequently used in satellite-based albedo retrieval from multi or single angle observations[15-16]. Therefore, it is an essential issue to understand what uncertainty induced by different BRDF smooth on albedo retrievals.

2 Data and Method

2.1 Data

Regions with rich land cover types and good public datasets in of North America was selected to serve the case study of this work. MCD12C1, MCD12Q1, MCD43A1, MCD43A3, MCD43C1, MCD43C3 and

* Corresponding author: 471910043@stu.lntu.edu.cn

other data sets of MODIS were used to provide classification, BRDF and albedo of land cover in 2019. These MODIS datasets were downloaded from <https://ladsweb.modaps.eosdis.nasa.gov/search/>.

This paper discussed the situation of land cover with no snow, as snow can not reflect the real situation of land cover and will cause great interference to spatiotemporal smoothing, so the DOYs (Day of year) with snow were removed from the data sets. In the operational products of MODIS albedo, there are two modes (full inversion and magnitude inversion) according to the observations. If it is magnitude inversion, the inversion quality of albedo is low, and there will be a certain difference from its true value, which will disturb the spatiotemporal

smoothing. Therefore, the albedo with low quality should be removed through the QA data layer in the data sets.

Through IGBP data layer in MODIS-MCD12C1, we selected DBF sample (-94.88°W & 31.23°N) with high confidence (93%) as study site, whose average slope is 2.84° and altitude is 59.71m. Then, the DBF sample at 5600m was re-projected to IGBP data layer in MODIS-MCD12Q1 (500m) to obtain more detailed classification result, and a representative sample at 500m spatial scale was selected from the homogeneous cushion. The MODIS pixel at 500m was used for temporal smoothing, while a spatial smoothing was carried out from 500m to 5600m. Fig. 1. shows the work follow of this study.

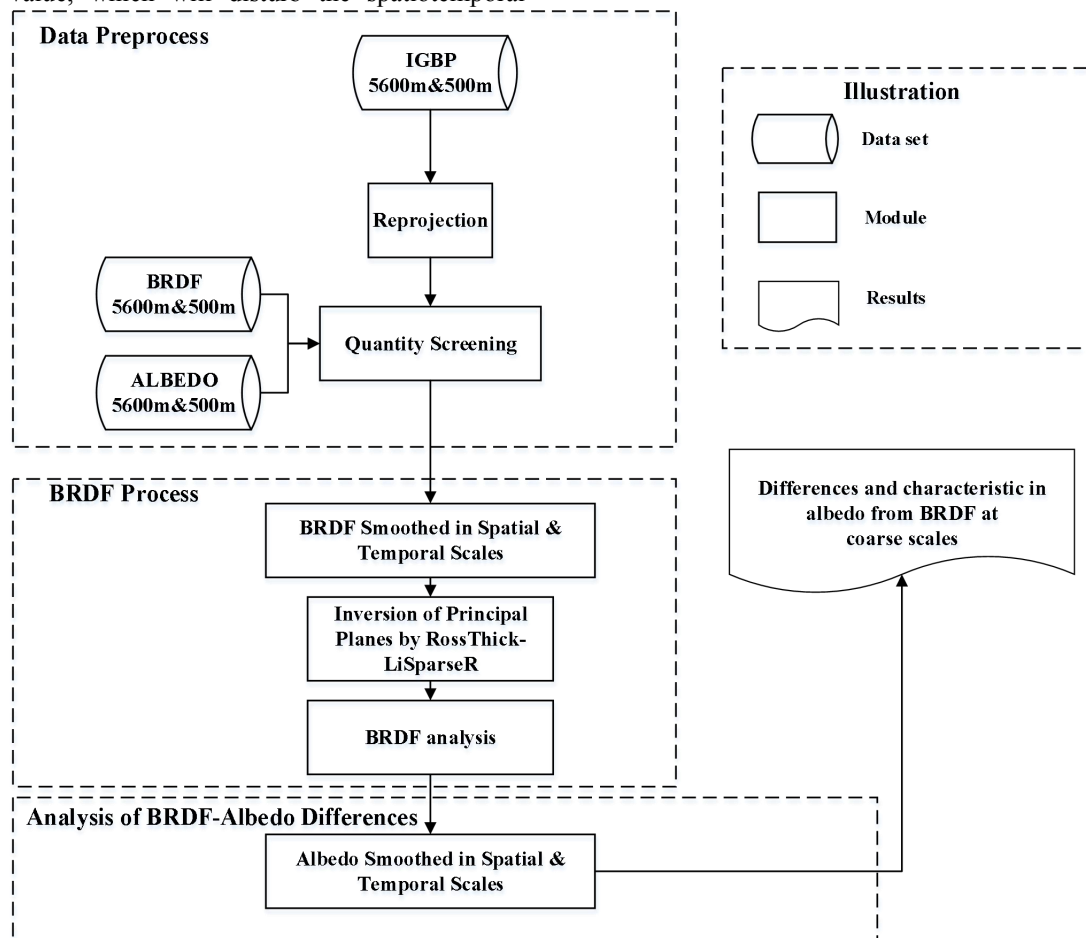


Fig. 1. Work flow chart

2.2 BRDF spatiotemporal smoothing

There are 3 work modules in Fig. 1: Data preprocess, BRDF process, Analysis of BRDF-Albedo differences. Data preprocess module has been discussed in section 2.1. In BRDF process module, as MODIS describes BRDF through a linear kernel driven model (RossThick-LiSparseR), a set of fixed kernel coefficients can determine a BRDF model and MODIS-BRDF products (MCD43C1 & MCD43A1) provide kernel coefficients, thus firstly BRDF parameters after spatiotemporal smoothing can represent the smoothed BRDF model;

then, reflectance with different incident-view geometry is retrieved by RossThick-LiSparseR model to obtain BRDF principle plane curve.

During the retrieval processing of albedo, albedo is a hemispherical integration of BRDF, so the magnitude and shape of BRDF principle plane curve have potential impact on albedo. In the reflecting hemisphere, the change of the principle plane (i.e. the plane determined by two lines from surface target respectively to observer and sun) is the most complex and representative. This principle plane can not only reflect the angle effect brought by the incident-view geometry, but also contains hot spot information, so it can best reflect the characteristics of BRDF. In this paper, negative values

less than 0 degree represent backward and positive values greater than 0 degree represent forward; Then, based on the differences of the reflectivity in the curves at direction of 0° , $\pm 45^\circ$, $\pm 70^\circ$, the STD (Standard Deviation) of feature points is taken as the shape difference coefficient. If difference coefficient is small, the shape changes of principle plane curves are small; otherwise, the shape changes are large. The difference of BRDF magnitudes were used to investigate the dispersion of the all BRDF principle plane curves.

2.3 Absolute and relative differences of albedo

To explore the differences caused by BRDF temporal smoothing on the retrieval of albedo. Firstly, the smoothed monthly values of albedo in 12 months of the year 2019 were calculated, and then the smoothed WSA values at 16-days and 8-days scales within one month were calculated; Lastly, the daily albedo values were compared with the corresponding smoothed albedo values in three broad bands: Near-Infrared(NIR), Short Wave(SW), Visible(VIS) and the relative & absolute differences were calculated. When discussing the influence of BRDF spatial smoothing on the retrieval of albedo, we extracted albedo at 500m and 5600m from MCD43A3 and MCD43C3 products, then calculated the relative & absolute differences between them, lastly we counted the daily differences throughout the year 2019 to explore the magnitudes of the differences.

3 Results and Discussion

3.1 Temporal smoothing of BRDF and related albedo

In order to explore the difference of BRDF before and after multi-temporal smoothing, the BRDF parameters of DBF sample at 500m were extracted from MCD43A1 product, then BRDF was smoothed according to multi-temporal scales(8 days, 16 days, month). To obtain the smoothed principal plane curve and daily principal plane curves of BRDF, reflectance was calculated under different incident-view geometry based on RossThick-

LiSparseR model and BRDF parameters before and after smoothing. Taking the growing season (March) and declining season (December) as an example (Fig. 2), this paper showed the differences of BRDF principle plane curves before and after temporal smoothing(day-month) in three broad bands of Near-Infrared(NIR), Short Wave(SW) and Visible(VIS). Meanwhile, the relative and absolute differences of albedo in March and December were counted (Table 1).

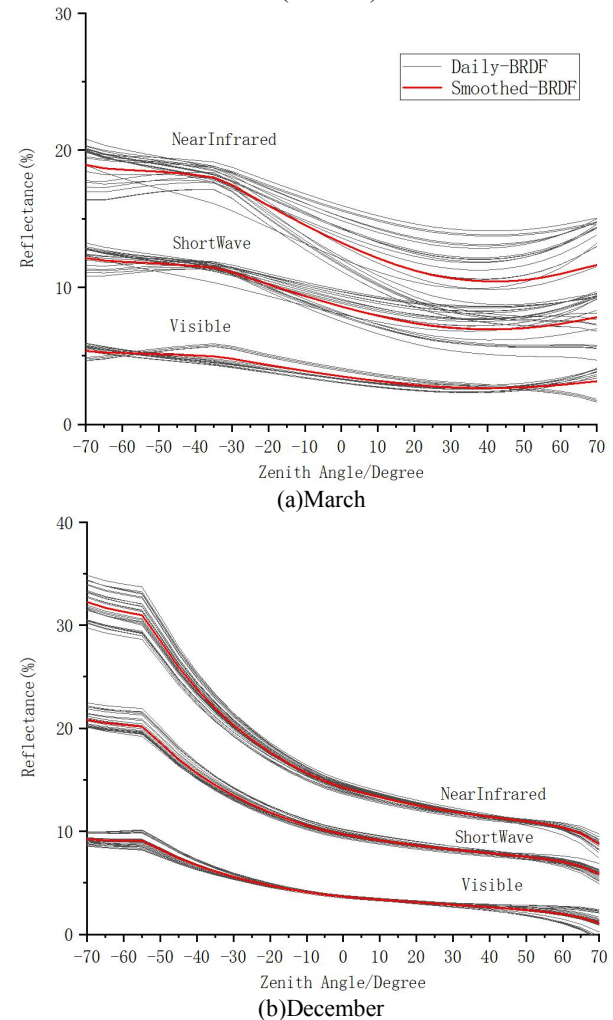


Fig. 2. BRDF before and after temporal smoothing

Table 1. The differences of principle plane curves' magnitudes and feature points before and after BRDF temporal smoothing

Band	Month	Magnitude(%)	Hotspot(%)	-45°(%)	-70°(%)	45°(%)	70°(%)	0°(%)	STD
NIR	3	1.42	0.50	0.62	1.27	2.11	3.02	1.36	0.87
	12	0.38	1.19	0.89	1.20	0.10	0.31	0.24	0.45
SW	3	0.71	0.21	0.25	0.73	1.08	1.80	0.63	0.54
	12	0.22	0.69	0.51	0.66	0.12	0.31	0.15	0.23
VIS	3	0.17	0.62	0.35	0.39	0.10	0.96	0.35	0.27
	12	0.04	0.46	0.29	0.32	0.19	0.70	0.05	0.20

Table 2. Albedo differences caused by BRDF temporal smoothing

Band	Month	Relative difference (%)	Absolute difference	Month	Relative difference (%)	Absolute difference
NIR	3	10.97	0.0172	12	1.80	0.0029

SW	3	9.42	0.0095	12	1.51	0.0016
VIS	3	8.24	0.0035	12	1.67	0.0007

It can be seen from Fig. 2 and Table 1 that after temporal smoothing, the magnitudes and shapes of BRDF principle plane curves had changed to some extent. In three broad bands of NIR, SW and VIS, the overall magnitude differences of BRDF principle plane curves in March (1.42%, 0.71% and 0.17%) are significantly higher than those in December (0.38%, 0.22% and 0.04%), it means the dispersion of BRDF in March is higher than that in December; From the analysis of the differences dispersion of feature points(STD, Standard Deviation), the more discrete of feature points, the more intense changes of the shapes of BRDF, so the STD in March (0.87, 0.54, 0.27) are significantly higher than those in December (0.45, 0.23, 0.20).

Table 2 showed the magnitudes of albedo differences caused by BRDF temporal smoothing in March and December, and the relative and absolute differences of albedo in March are significantly higher than those in December. We selected the WSA(White Sky Albedo) from MCD43A3 data set as the processing object, as WSA is highly related to BSA(Black Sky Albedo) and has nothing to do with LSN(Local Solar Noon), so there

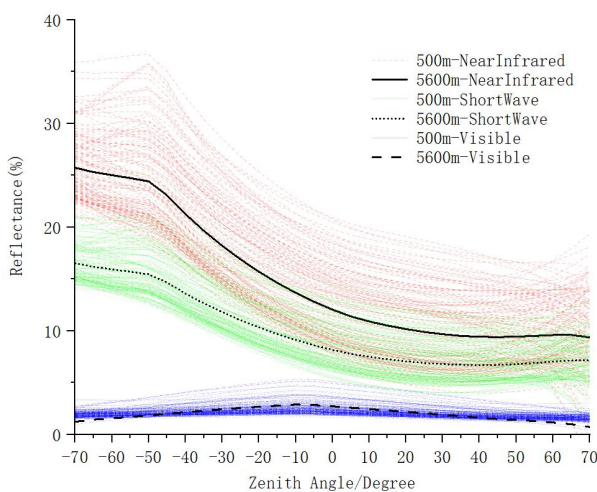
is no need to consider the difference caused by LSN[17-18].

3.2 Spatial smoothing of BRDF and related albedo

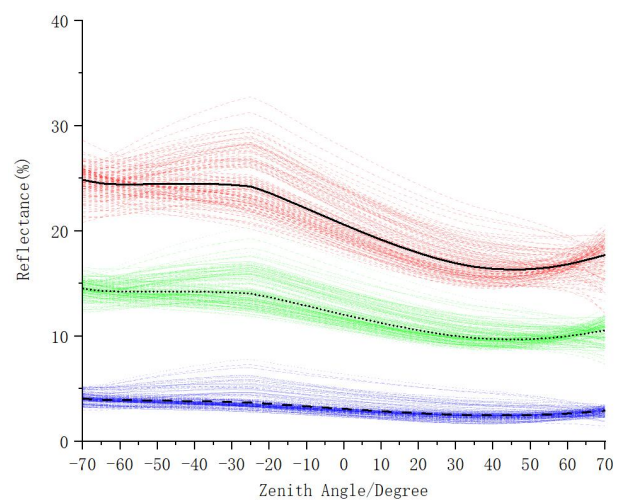
To explore the differences of BRDF before and after spatial smoothing, the BRDF parameters of DBF sample at 5600m were extracted from MCD43C1 product, then BRDF parameters of land cover at 500m were extracted from MCD43A1 product. The BRDF principle plane curves and albedo values at two spatial scales were retrieved based on RossThick-LiSparseR model, then the daily differences of BRDF and albedo were counted. For the DOYs with extreme difference after albedo spatial smoothing (from 500m to 5600m) in 2019 (Doy1-365), statistics were made on the BRDF principle plane curves in three broad bands of NIR, SW and VIS(Fig. 3). We also made statistics of the albedo differences on the DOYs with extreme albedo difference(Table 3) and the changes of BRDF principle plane curves on the extreme DOYs(Table 4).

Table 3. Statistics of DOYs with extreme differences

Site	Band	Term	DOY	Relative Difference (%)	Absolute Difference
DBF	NIR	MAX	33	17.38	0.0250
		MIN	98	4.31	0.0104
	SW	MAX	32	14.38	0.0139
		MIN	99	4.22	0.0059
	VIS	MAX	158	27.23	0.0052
		MIN	93	8.31	0.0032



(a) Maximum DOYs



(b) Minimum DOYs

Fig. 3. Distribution of BRDF principle plane curves in extreme DOYs

Table 4. The differences of principle plane curves' magnitudes and feature points before and after BRDF smoothing

Band	Term	Magnitude(%)	Hotspot(%)	-45°(%)	-70°(%)	45°(%)	70°(%)	0°(%)	STD
NIR	MAX	2.90	3.87	3.72	2.71	2.83	3.23	3.22	0.42
	MIN	1.27	2.19	1.46	1.07	1.04	1.37	1.71	0.39
SW	MAX	1.63	2.21	2.13	1.59	1.54	1.86	1.81	0.25
	MIN	0.76	1.35	0.92	0.62	0.59	0.83	1.02	0.25
VIS	MAX	0.29	0.67	0.29	0.73	0.35	0.90	0.56	0.21
	MIN	0.39	0.60	0.47	0.36	0.35	0.28	0.47	0.11

It can be seen from Fig. 3 and Table 3&4 that after spatial smoothing, the magnitudes and shapes of BRDF had changed to some extent. The dispersion of feature points(STD) and overall magnitude differences are both impact factors to the differences. In the three broad bands of NIR, SW and VIS, the STD on maximum DOYs are almost larger than that on minimum DOYs; In the SW band where the maximum DOY and the minimum DOY are almost the same, but the magnitude of maximum DOY is significantly greater than that of minimum DOY.

4 Conclusion

The magnitudes and shapes of BRDF in principle planes are changed significantly after smoothing at multi-spatiotemporal scales, and it can induce detectable differences for the inversed albedo. As the case study of DBF sample, BRDF smoothed from day to month lead to relative differences to smoothed values of 10.97%, 9.42%, 8.24% and absolute differences of 0.0172, 0.0095 and 0.0035 on the estimated albedo respectively at Near-Infrared, Short Wave and Visible broad bands. The BRDF smoothed at spatial scale from 500m to 5600m results in relative differences to smoothed values of 17.38%, 14.38%, 27.23% and absolute differences of 0.0250, 0.0139, 0.0052 respectively on retrieved albedo at three above broad bands.

This work was supported by the National Natural Science Foundation of China (No. 42071351), the National Key Research and Development Program of China (No. 2020YFA0608501, No. 2017YFB0504204), the Liaoning Revitalization Talents Program (No. XLYC1802027), Talend recruited program of the Chinese Academy of Science (No. Y938091), Project supported discipline innovation team of Liaoning Technical University (No. LNTU20TD-23)

References

1. J.T. Kiehl, J.J. Hack, G.B. Bonan, et al. Description of the NCAR Community Climate Model (CCM3). National Center for Atmospheric Research Publishing, The Boulder (1996).
2. B. Pinty, T. Lavergne, T. Kaminski, et al. Partitioning the solar radiant fluxes in forest canopies in the presence of snow. *Journal of Geophysical Research*, **113** D04104 (2008)
3. D.S. Kimes and P.J. Sellers, Inferring Hemispherical Reflectance of the Earth's Surface for Global Energy Budgets from Remotely Sensed Nadir of Directional

Radiance Values. *Remote Sensing of Environment*, **18**: 205–223 (1985)

4. D.S. Kimes, P.J. Sellers and W.W. Newcomb, Hemispherical Reflectance Variations of Vegetation Canopies and Implications for Global and Regional Energy Budget Studies. *Journal of Climate and Applied Meteorology*, **26**: 959–972 (1987)
5. A. Henderson and M. Wilson., Surface albedo data for climatic modeling. *Reviews of Geophysics*. **21**: 1743–1778 (1983)
6. P. Sellers, B. Meeson, F. Hall, et al. Remote sensing of the land surface for studies of global change: Models-Algorithms-Experiments. *Remote Sensing of Environment*, **51**: 3–26 (1995)
7. Z. Wang, C. Schaaf, Q. Sun, et al. Capturing rapid land surface dynamics with Collection V006 MODIS BRDF/NBAR/Albedo (MCD43) products. *Remote Sensing of Environment*, **207** 50-64 (2018)
8. Z. Wang, A. Erb, C. Schaaf, et al. Early spring post-fire snow albedo dynamics in high latitude boreal forests using Landsat-8 OLI data. *Remote sensing of environment*, **185**: 71-83 (2016)
9. P. Lewis, et al. The ESA globAlbedo project: Algorithm. In: 2012 IEEE International Geoscience and Remote Sensing Symposium. Munich. 5745-5748 (2012)
10. W. Lucht, C. Schaaf and A. Strahler, An algorithm for the retrieval of albedo from space using semiempirical BRDF models. *IEEE TRANSACTIONS ON GEOSCIENCE AND REMOTE SENSING*, **38** 977–998 (2000)
11. C. Schaaf, F. Gao, A. Strahler, et al. First operational BRDF, albedo nadir reflectance products from MODIS. *Remote Sensing of Environment*, **83**: 135–148 (2002)
12. C. Bacour and F. Bréon, Variability of biome reflectance directional signatures as seen by POLDER. *Remote Sensing of Environment*, **98** 80-95 (2005)
13. S. Liang, X. Zhao, S. Liu, et al. A long-term Global Land Surface Satellite (GLASS) data-set for environmental studies. *International Journal of Digital Earth*, **6** 5-33 (2013)
14. Q. Liu, L. Wang, Y. Qu, et al. Preliminary evaluation of the long-term GLASS albedo product. *International Journal of Digital Earth*, **6**: 69-95 (2013)
15. Y. Shuai, J. Masek, F. Gao, et al. An algorithm for the retrieval of 30-m snow-free albedo from Landsat

- surface reflectance and MODIS BRDF. Remote Sensing of Environment, **115** 2204-2216 (2011)
16. Y. Shuai, J. Masek, F. Gao, et al. An Approach for the Long-Term 30-m Land Surface Snow-Free Albedo Retrieval from Historic Landsat Surface Reflectance and MODIS-based A Priori Anisotropy Knowledge. Remote Sensing of Environment, **152** 467-479 (2014)
 17. Y.H. Zheng, L. Huang and J. Zhai, Impacts of land cover changes on surface albedo in China,the United States,India and Brazil. Journal of Remote Sensing(Chinese), **24**: 917-932 (2020)
 18. H. Zhang, Z.T. Jiao, D.Y. Dong, et al. Albedo retrieved from BRDF archetype and surface directional reflectance. Journal of Remote Sensing(Chinese), **19** 355-367 (2015)